2007 IEEE International Conference on
Robotics and Automation
Roma, Italy, 10-14 April 2007

A Powered Leg Orthosis for Gait Rehabilitation of Motor-Impaired Patients

Sai K. Banala, Alexander Kulpe and Sunil K. Agrawal

Abstract— **This paper describes a powered leg orthosis for gait rehabilitation of patients with walking disabilities. The paper proposes controllers which can apply suitable forces on the leg so that it moves on a desired trajectory. The description of the controllers, simulations and experimental results with the powered orthosis are presented in the paper. Currently, experiments have been performed with a dummy leg in the orthosis. In the coming months, this powered orthosis will be used on healthy subjects and stroke patients.**

I. Introduction

Profound muscle weakness or impairment in motor control affects a vast number of people, especially resulting from neurological injury, such as hemiparesis from stroke. The patients often have substantial limitations on movement. Rehabilitation after stroke helps to improve the walking function. Robotic rehabilitation has many advantages over conventional manual rehabilitation. Some of these are: (i) robotic rehabilitation may reduce burden on clinical staff, (ii) interaction forces and torques, measured with various sensors, can assess quantitatively the level of motor recovery and (iii) robotics can help in delivering well controlled repetitive training sessions at reasonable cost.

Currently, available lower extremity orthotic devices can be classified as either passive, where the human subject applies forces to move the leg, or active, where actuators on the device apply forces on the human leg. One of the passive devices is gravity balancing leg orthosis, developed at University of Delaware [1]. T-WREX [2] is an upper extremity passive gravity balancing device. Passive devices cannot supply energy to the leg, hence are limited in their ability compared to active devices. Lokomat is an actively powered exoskeleton, designed for patients with spinal cord injury. A patient uses this machine while walking on a treadmill [3]. Mechanized Gait Trainer (MGT) is a single degree-of-freedom powered machine that drives the leg to move in a prescribed gait pattern. The machine consists of a foot plate connected to a crank and rocker system. The device simulates the phases of gait, supports the subjects according to their ability, and controls the center of mass in the vertical and horizontal directions [4]. AutoAmbulator is a rehabilitation machine for the leg to assist individuals with stroke and spinal cord injuries. This machine is designed to replicate the pattern of normal gait [5]. HAL [6] is a powered suit for elderly people and persons with gait deficiencies which takes EMG signals as input and produces appropriate torque to perform the task. Another power assisted exoskeleton is BLEEX, Berkeley lower extremity exoskeleton [7]. It is not intended to be a rehabilitation device, but a human strength multiplier. PAM (Pelvic Assist Manipulator) is an active device for assisting the human pelvis to allow more natural motion [8]. There are a variety of active devices that target a specific disability or weakness in a particular joint of the leg ([9], [10], [11], [12], [13]). A limiting feature of the machines like AutoAmbulator is that they move patients through predetermined movements rather than allowing them to move under their own control. The failure to allow patients to experience and practice appropriate movement patterns prevents necessary changes in the nervous system for relearning. Forced motion along a fixed trajectory might result in "learned helplessness" which could be sub-optimal [14]. However, at this time, devices which can apply appropriate forces to to the leg to help in gait rehabilitation, are still under development.

In this paper, we propose a powered lower extremity orthosis (Fig. 1) and controllers based on application of force fields. The goal of these controllers is to assist or resist the motion of the leg, as needed, by applying force-fields around

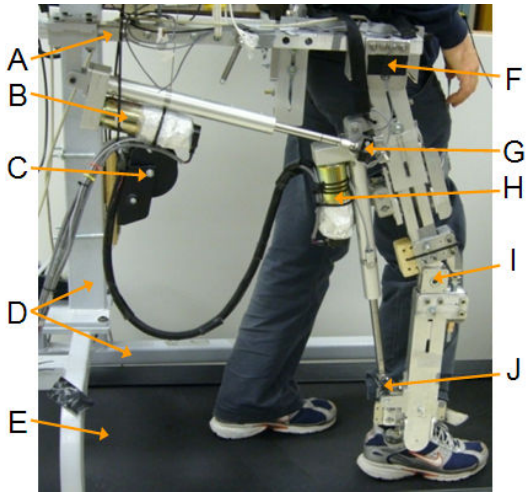

Fig. 1. Powered leg orthosis with a human subject. A: boom to support hip motor, B: hip linear actuator, C: spring-loaded winch to support device weight, D: walker to support the device, E: treadmill F: hip joint, G: load-cell on hip linear-actuator, H: knee linear actuator, I: knee joint J: load-cell on knee linear actuator.

Sai K. Banala: Graduate Student, Mechanical Systems Laboratory, Department of Mechanical Engineering, University of Delaware, Newark, DE 19716, U.S.A. sai@udel.edu

Alexander Kulpe: Graduate Student, Mechanical Systems Laboratory, Department of Mechanical Engineering, University of Delaware, Newark, DE 19716, U.S.A. kulpe@udel.edu

S. K. Agrawal: Professor, Mechanical Systems Laboratory, Department of Mechanical Engineering, University of Delaware, Newark, DE 19716, U.S.A. agrawal@udel.edu

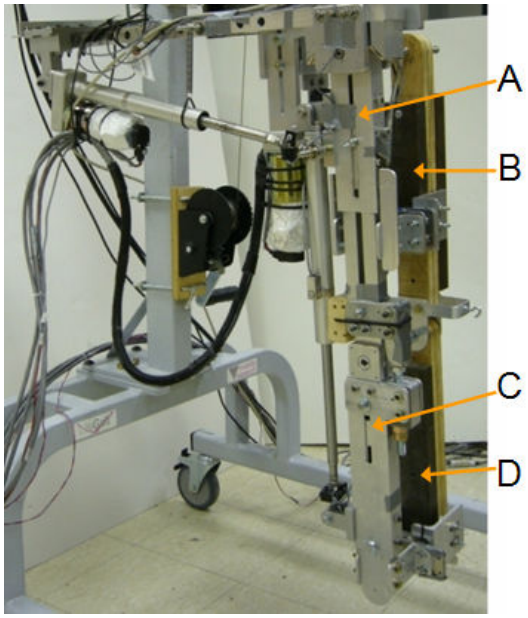

Fig. 2. Powered leg orthosis with a dummy leg. A: device thigh, B: dummy leg thigh, C: device shank, D: dummy leg shank.

the leg. The user is not restricted to a desired trajectory. The controllers implemented to achieve these goals are (1) trajectory tracking control, (2) set-point control and (3) force-field control. Trajectory tracking control moves the leg in a fixed trajectory, which is not desirable for gait training. Set-point control and force-field control use the concept of assistive force as needed, which is desirable.

II. Orthosis Design

A. Device Description

The design of the active orthosis is based on our prototype of passive Gravity Balancing Leg Orthosis [1]. The orthosis is connected to a walker and its trunk has four degrees-of-freedom (dof) with respect to the walker. These dof are vertical and lateral translation, rotation about vertical axis and horizontal axis perpendicular to sagittal plane. Hip joint of the orthosis has two dof with respect to the trunk, one in sagittal plane and the other for abduction-adduction motion. Knee has one dof with respect to the thigh segment. The device also has a foot segment attached to the shank of the leg, with one dof ankle joint. The foot support allows inversion-eversion motion to the ankle due to its structural design. The hip joint in the sagittal plane and knee joint are actuated using linear motors. These motors have encoders built into them, which are used to find the joint angles. The physical interface between the orthosis and the dummy/human leg is through two force-torque sensors, one mounted between thigh segments of the orthosis and the leg, the other mounted between shank segments of the orthosis and the leg.

The ankle segment described above is used when a human subject is in the device. During initial testing, we use a dummy leg (Fig. 2), which does not have a foot segment.

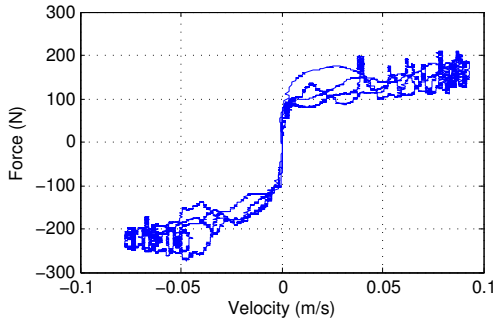

Fig. 3. Frictional force in a linear actuator as a function of its linear velocity.

B. Control Architecture

The controllers developed for the orthosis are (1) Trajectory Tracking Controller, (2) Set-point PD controller and (3) Force-Field controller. In trajectory tracking controller, desired trajectory $\theta_d(t)$ is a prescribed function of time, whereas in set-point PD control, a finite number of desired set-points is used. Current set-point moves to the next point only when the current position is within a given tolerance region around the current set-point. Both the trajectory tracking controller and set-point PD controller use feedback linearized PD control in joint space. In a force-field controller, the forces are applied at the foot to create a tunnel or virtual wall-like force field around the foot. The patient using the orthosis for rehabilitation is then asked to move the leg along this tunnel. The set-points for the controller are chosen such that the density of points is higher in the regions of higher path curvature in the foot space.

Since the orthosis uses linear electrical motors, they have substantial friction in the gearing. To overcome this friction we use the following methods [15]; (1) Model based compensation, in which we feed-forward frictional forces to the controller using a friction model obtained from experiments; (2) Load-cell based compensation, in which we use load-cells in-line with the lead screw of the linear motor along with a fast PI controller. We have also studied the use of an adaptive friction controller, we observed that the adaptive identification does not work well during external contact [16]. Using direct-drive motors we could completely eliminate the problem of friction, but considering the torque and motor weight requirements we had to choose a linear actuator.

C. Friction Compensation

For feed-forward friction compensation, we need a good friction model. Fig. 3 shows the frictional force data collected by experiment from a motor as a function of its linear velocity. The plot has ripples in the first and third quadrants. This behavior can be approximated with the equation $F_{friction} = K_{fs}\,\text{sign}(\dot{x}) + K_{fd}\dot{x}$, where $\dot{x}$ is the linear velocity of the motor, K_{fs} and K_{fd} are constants.

The friction model is only an approximation and the actual friction has a complicated dependency on the load applied to the motor and on the configuration of the device [17], [18].

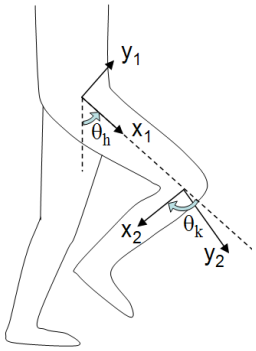

Fig. 4. Schematic showing anatomical joint angle convention.

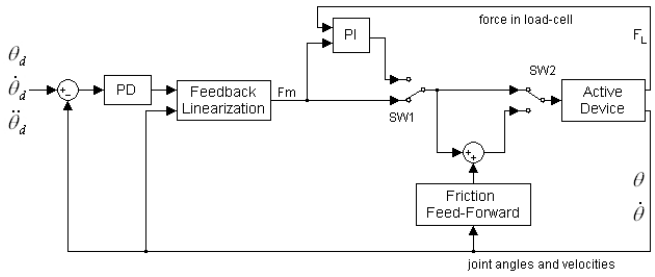

Fig. 5. PD Controller. $\boldsymbol{\theta}$ is the current joint angles, $\boldsymbol{\theta}_d$ is the desired trajectory and $\mathbf{F_L}$ is the force measured by the load-cell. For set-point control, $\dot{\boldsymbol{\theta}}_d$and $\ddot{\boldsymbol{\theta}}_d$ are zero. Switch SW1 turns on load-cell based friction compensation and switch SW2 turns on model based friction compensation.

Some of the problems of model based friction compensation can be overcome by using a load-cell in series and a fast PI controller with a suitable time constant [16].

III. Trajectory Tracking Controller

Trajectory tracking controller tracks the desired trajectory using a feedback linearized PD controller. This controller is simple and is robust to friction with higher feedback gains. When used with friction compensation, small feedback gains can be used. Fig. 5 shows the schematic of the trajectory tracking PD control. In the figure, switch SW1 turns on the load-cell based friction compensation and switch SW2 turns on the model based friction compensation.

In this trajectory tracking controller, the desired trajectory in terms of joint angles is a function of time, $\boldsymbol{\theta}_d = \boldsymbol{\theta}_d(t)$. The desired trajectory was obtained from healthy subject walking data, using experiments with our passive device [1]. The equations of motion for the device are given below, note that the frictional terms are not mentioned here as they are assumed to be compensated using one of the two friction compensation methods outlined in Sec. II-C.

$$\mathbf{M}\ddot{\boldsymbol{\theta}} + \mathbf{C}(\dot{\boldsymbol{\theta}}, \boldsymbol{\theta})\dot{\boldsymbol{\theta}} + \mathbf{G}(\boldsymbol{\theta}) = \tau\,, \tag{1}$$

where $\mathbf{M}$ is the inertia matrix, $\mathbf{C}$ is the matrix with centrifugal and Coriolis terms and $\mathbf{G}$ has gravity terms. $\boldsymbol{\theta} = [\theta_h\ \theta_k]^T$ shown in Fig. 4. Control law is given by:

$$\tau = \mathbf{M}(\ddot{\boldsymbol{\theta}}_d + \mathbf{K}_d\dot{\boldsymbol{\theta}}_e + \mathbf{K}_p\boldsymbol{\theta}_e) + \mathbf{C}(\dot{\boldsymbol{\theta}}, \boldsymbol{\theta})\dot{\boldsymbol{\theta}} + \mathbf{G}(\boldsymbol{\theta})\,,$$

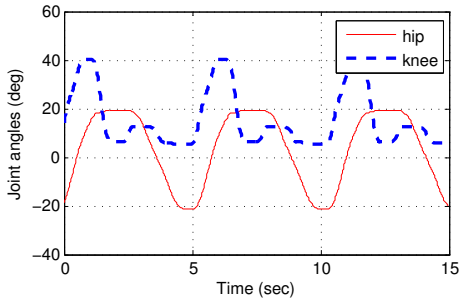

Fig. 6. Experimental results showing joint angles of dummy leg obtained with trajectory tracking controller.

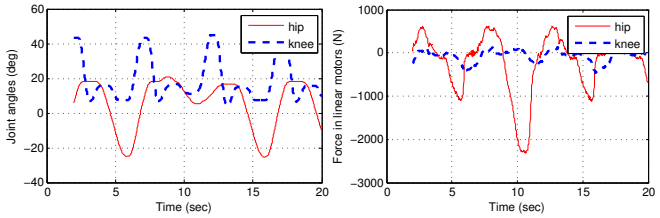

(a) Joint angles (b) Force in motors

Fig. 7. Plots showing joint angles in (a) and corresponding forces in linear motors in (b). Note that at around 10 seconds, the hip joint is prevented from crossing 0 degree by applying external forces, as a result the force applied by the hip motor almost doubled.

where $\boldsymbol{\theta}_e = \boldsymbol{\theta}_d - \boldsymbol{\theta}$. This law linearizes the equations to an exponentially stable system:

$$\ddot{\boldsymbol{\theta}}_e + \mathbf{K}_d\dot{\boldsymbol{\theta}}_e + \mathbf{K}_p\boldsymbol{\theta}_e = 0 \tag{2}$$

where $\mathbf{K}_p = \begin{pmatrix} K_{p1} & 0 \\ 0 & K_{p2} \end{pmatrix}$ and $\mathbf{K}_d = \begin{pmatrix} K_{d1} & 0 \\ 0 & K_{d2} \end{pmatrix}$ and are positive matrices.

A. Simulations and Experiments

Figure 6 shows the joint angles obtained with the trajectory tracking controller. When friction compensation was not used, the feed back gains were: $K_{p1} = 300, K_{p2} = 525.5, K_{d1} = 33, K_{d2} = 5.8$. When load-cell based compensation was used the feedback gains were: $K_{p1} = 45, K_{p2} = 66, K_{d1} = 10.8, K_{d2} = 5.0$. This shows that one way to use small feedback gains is to use friction compensation.

Since the desired trajectory is a function of time, the error in any joint keeps on increasing if that joint is prevented from moving. This causes the force in the motor of that joint to increase with the error. Fig. 7(a) shows joint angles of the dummy leg with trajectory tracking controller, at around 10 seconds, the hip joint is prevented from crossing 0 degrees by applying external forces, as a result, the force in the hip motor almost doubled. This increase in forces when the subject wishes not to move their leg might not be safe or suitable for training.

IV. Set-Point PD Controller

Set-point PD controller is similar to trajectory tracking controller except that there are a finite number of desired trajectory points $(\boldsymbol{\theta}_{d1}, \boldsymbol{\theta}_{d2}, ..., \boldsymbol{\theta}_{dn})$ and desired trajectory

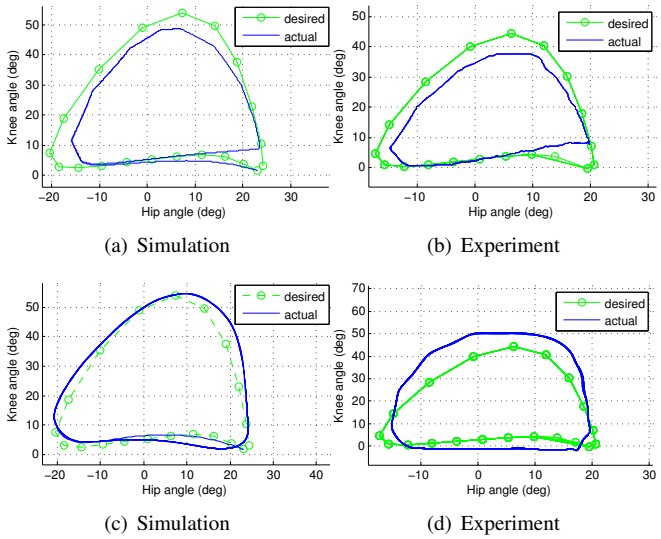

(a) Simulation (b) Experiment

(c) Simulation (d) Experiment

Fig. 8. Simulation and experimental results showing joint angles, for set-point controller. For (a) and (b) ω_n =10.12, ξ =3.2, For (c) and (d): ω_n =10.12, ξ =0.5

velocities and accelerations are set to zero ($\dot{\boldsymbol{\theta}}_d = \ddot{\boldsymbol{\theta}}_d = 0$). The controller takes the device to the current set-point. Once the current position of the device is close to the current set-point, the current set-point is switched to the next set-point. If the number of set-points is small, the device motion is jerky. However by choosing enough number of points, the leg trajectory can be made to be smooth.

One of the advantages of set-point PD controller over trajectory tracking controller is that if the human subject wishes to stop the device, the forces on the leg stays within limit. The set-point will not change.

The control law is same as the one used in trajectory tracking PD controller with desired trajectory velocities and accelerations set to zero $\dot{\boldsymbol{\theta}}_d = \ddot{\boldsymbol{\theta}}_d = 0$. The current set-point $\boldsymbol{\theta}_{cur} = \boldsymbol{\theta}_i$ advances to the next set-point $\boldsymbol{\theta}_{i+1}$ if $\|\boldsymbol{\theta} - \boldsymbol{\theta}_{cur}\| \leq \epsilon$, where ϵ is the allowed tolerance.

A. Simulation and Experiments

Simulations and experiments were performed for thee sets of feedback gains. These gains were chosen such that the natural frequency of the system described in Eq. (2) is ω_n =10.12 and ξ ={3.2, 0.5}.

Figures 8 show the simulation and experimental results of the joint angle trajectory with hip-joint angle along x-axis and knee joint angle on the y-axis. We can note that for larger values of damping, the joint trajectories lie inside the desired trajectory due to slowing effects of damping. At lower values of damping, the trajectories fluctuate around the desired trajectory due to faster speeds and overshoots. The difference between the plots can be attributed to the inexact mathematical model used in the simulation and experiments in the parameter estimation.

V. Force-Field Controller

The goal of the force-field controller is to create a force field around the foot in addition to providing damping to

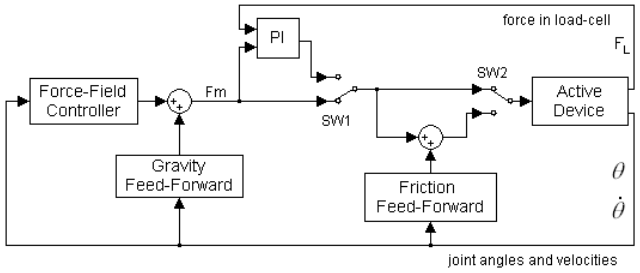

Fig. 9. Force-Field Controller. $\mathbf{F_L}$ is the force measured by the load-cell. Switch SW1 turns on sensor based friction compensation and switch SW2 turns on model based friction compensation.

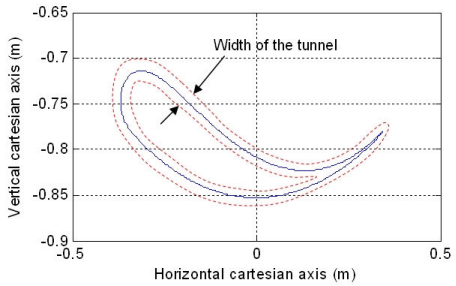

Fig. 10. Cartesian plot of the foot in the trunk reference frame, origin set at the hip joint. The solid line (in blue) is the desired trajectory of the foot and the dashed lines (in red) are the virtual walls.

it. This force field is shaped like a "virtual tunnel" along the desired trajectory. Fig. 9 shows the basic structure of the controller. This controller uses gravity compensation to help the human subject. This assistance can be reduced or completely removed if required. Fig. 10 shows typical shape of tunnel walls around the desired trajectory.

Since the virtual tunnel is used to guide the foot of the subject, the forces are applied on the foot. These forces are a combination of tangential force $\mathbf{F}_t$, normal force $\mathbf{F}_n$ to the desired trajectory and damping force $\mathbf{F}_d$. We designed the controller such that this normal component keeps the foot within the virtual tunnel. The tangential force provides the force required to move the foot along the tunnel in forward direction. And the damping force is to minimize oscillations.

Let $\mathbf{P}$ be the current position of the foot in the Cartesian space in the reference frame attached to trunk of the subject, $\mathbf{N}$ be the nearest point to $\mathbf{P}$ on the desired trajectory, $\hat{\mathbf{n}}$ is the normal vector from $\mathbf{P}$ to $\mathbf{N}$, $\hat{\mathbf{t}}$ is the tangential vector at $\mathbf{N}$ along the desired trajectory in forward direction. The force $\mathbf{F}$ on the foot is defined as:

$$\mathbf{F} = \mathbf{F}_t + \mathbf{F}_n + \mathbf{F}_d \tag{3}$$

where $\mathbf{F}_t$ is the tangential force, $\mathbf{F}_n$ is the normal force and $\mathbf{F}_d$ is the damping force. The tangential force $\mathbf{F}_t$ is defined as:

$$\mathbf{F}_t = \begin{cases} K_{Ft}(1 - d/D_t)\hat{\mathbf{t}} & if\ d/D_t < 1 \\ 0 & otherwise \end{cases} \tag{4}$$

The normal force $\mathbf{F}_n$ is given by:

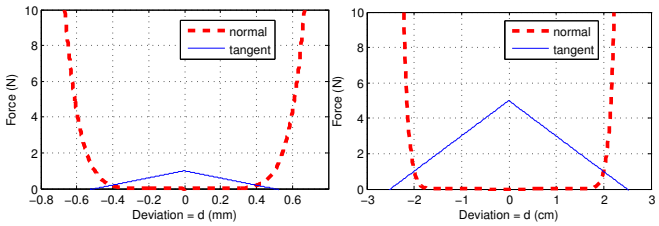

(a) Narrow tunnel (b) Wider tunnel

Fig. 11. Tangential and normal forces as a function of distance from the desired trajectory, positive force points towards the trajectory. Parameters used are: (a) $K_{Ft} = 1, D_n = 0.0005, D_t = 0.0005, n = 3$, (b) $K_{Ft} = 1, D_n = 0.02, D_t = 0.025, n = 10$

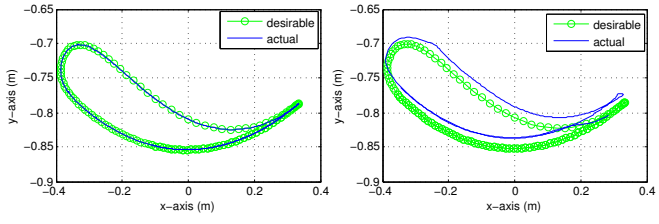

(a) Narrow tunnel (b) Wider tunnel

Fig. 12. Simulation results of force-field controller showing foot trajectory in Cartesian frame attached to the trunk, origin set at hip joint.

$$\mathbf{F}_n = \left(\frac{d}{D_n}\right)^{2(n+1)} \hat{\mathbf{n}} \tag{5}$$

The damping force $\mathbf{F}_d$ on the foot to reduce oscillations is given by:

$$\mathbf{F}_d = -K_d \dot{\mathbf{x}} \tag{6}$$

where K_{Ft}, D_t, D_n and K_d are constants, d is the distance between the points **P** and **N.** $\dot{\mathbf{x}}$ is the linear velocity of the foot.

The shape of the tunnel is given by Eq. (5). Higher the value of n, steeper are the walls. Also, at higher values of n, the width of the tunnel gets closer to D_n. Fig. 11 shows plots of tangential and normal forces as a function of distance d from the desired trajectory, positive force points towards the trajectory. Note that the tangential force ramps down as the distance d increases. This is to bring the leg closer to the trajectory before applying tangential force.

The required actuator inputs at the leg joints that apply the above force field $\mathbf{F}$ is given by:

$$\tau_m = \begin{bmatrix} \tau_{m1} \\ \tau_{m2} \end{bmatrix} = \mathbf{J}^T \mathbf{F} + \mathbf{G}(\boldsymbol{\theta}), \tag{7}$$

where $\mathbf{G}(\boldsymbol{\theta})$ is for gravity compensation. Finally, the forces in the linear motors $\mathbf{F}_m = [F_{m1},\ F_{m2}]$ are computed using the principle of virtual work, given by $\mathbf{F}_{mi} = \frac{\dot{\theta}_i}{\dot{l}_i}\tau_{mi},\ i = 1, 2$, where l_i is the length of i^{th} linear motor. The proof of stability for this controller is given in the appendix.

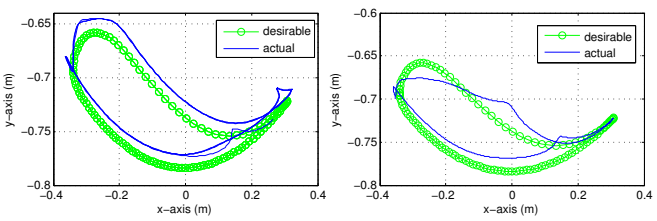

(a) Simulation result (b) Experimental result

Fig. 13. Results of force-field controller showing foot position in cartesian frame attached to the trunk of the subject with origin at the hip joint.

A. Simulations

Simulations were performed using the parameters shown in Fig. 11. We can see in Fig. 12 that with a narrow virtual tunnel, the error in the desired trajectory and the trajectory achieved is small when compared to the wider virtual tunnel. This shows that the maximum deviation of the foot from the desired trajectory can be controlled using the width of the tunnel D_n as the parameter. For least error in tracking, ideally D_n should be zero, but below certain value, the error won't decrease due to physical limitations of the device like motor torque saturation. When K_{Ft} is increased from 40 to 60, and all other parameters kept the same ($D_n = 0.02, D_t = 0.025, n = 10$), the tangential force also increases. As a result, the gait cycle period reduced from 5.0 seconds to 3.8 seconds. Thus K_{Ft} can be used as a parameter to change the gait time period.

B. Experimental results

The experiments with force field controller were conducted with dummy leg in the device. Experiments with a human subject are currently in progress. The parameters used were: $K_{Ft} = 50, D_n = 0.012, D_t = 0.025, n = 3$.

Figure. 13 shows plot of foot trajectory obtained from experiment and through simulation with the same set of parameters. Again, the difference between them could be attributed to the inexact mathematical model used in the simulation. In the figures, one can see the foot bouncing off the virtual tunnel walls.

VI. Conclusions and Future Work

Powered leg orthosis has been built, following the design of our passive leg device. It has linear actuators at hip joint and knee joints, it is also instrumented with force-torque sensors and encoders. Three types of controllers were implemented for the orthosis (1) trajectory tracking PD controller (2) set-point PD controller (3) force-field controller. All these controllers can be used with either (1) model based or (2) load-cell based friction compensation. We found that load-cell based friction compensation works better than model based compensation. Simulation and experimental results using all three controllers were presented. Simulation and experimental results show us that the set-point controller and force-field controller can apply forces that are more suitable for training, as the forces do not increase when the subject wishes to stop the motion of his leg. The applied forces can

assist desirable motion and resist undesirable motion of the leg, and are suitable for rehabilitation of lower extremity stroke patients.

Currently, healthy subject testing of force-fields controller is in progress. In future, we will use set-point and force-field controllers in rehabilitation of stroke patients.

VII. Acknowledgments

We gratefully acknowledged the support of NIH grant # 1 RO1 HD38582-01A2, help of Mr. Vivek Sangwan in machining some parts of the device and thanks to Dr. H. Pota for helpful discussions in the development of the controllers.

References

[1] S. K. Banala, S. K. Agrawal, A. Fattah, J. P. Scholz, V. Krishnamoorthy, K. Rudolph, and W.-L. Hsu, "Gravity balancing leg orthosis and its performance evaluation," *IEEE Transactions on Robotics*, vol. 22, no. 6, pp. 1228–1239, dec 2006.

[2] T. Rahman, W. Sample, and R. Seliktar, "Design and testing of wrex," in *presented at The Eighth International Confrence on Rehabilitation Robotics*, Kaist, Daejeon, Korea, 2003.

[3] G. Colombo, M. Joerg, R. Schreier, and V. Dietz, "Treadmill training of paraplegic patients using a robotic orthosis," *Journal of Rehabilitation Research and Development*, vol. 37, no. 6, 2000.

[4] S. Hesse and D. Uhlenbrock, "A mechanized gait trainer for restoration of gait," *Journal of Rehabilitation Research and Development*, vol. 37, no. 6, 2000.

[5] "Autoambulator," On the WWW, uRL http://www.autoambulator.com.

[6] H. Kawamoto and Y. Sankai, "Power assist system hal-3 for gait disorder person," in *International Conference on Computers for Handicapped Persons*, vol. 2398, 2002, pp. 196–203.

[7] P. Neuhaus and H. Kazerooni, "Design and control of human assisted walking robot," in *the IEEE International Conference on Robotics and Automation*, vol. 1, 2000, pp. 563–569.

[8] D. Aoyagi, W. E. Ichinose, S. J. Harkema, D. J. Reinkensmeyer, and J. E. Bobrow, "An assistive robotic device that can synchronize to the pelvic motion during human gait training," in *IEEE, International Conference on Rehabilitation Robotics*, 2003, pp. 565 – 568.

[9] E. Rocon, A. Ruiz, J. Pons, J. Belda-Lois, and J. S´anchez-Lacuesta, "Rehabilitation robotics: a wearable exo-skeleton for tremor assessment and suppression." in *IEEE, International Conference on Robotics and Automation*, 2005, pp. 2283–2288.

[10] J. Nikitczuk and B. W. andConstantinos Mavroidis, "Rehabilitative knee orthosis driven by electro-rheological fluid based actuators," in *IEEE, International Conference on Robotics and Automation*, 2005, pp. 2294–2300.

[11] G. S. Sawicki, K. E. Gordon, and D. P. Ferris, "Powered lower limb orthoses: applications in motor adaptation and rehabilitation," in *IEEE, International Conference on Rehabilitation Robotics*, 2005, pp. 206 – 211.

[12] J. F. Veneman, R. Ekkelenkamp, R. Kruidhof, F. C. T. van der Helm, and H. van der Kooij, "Design of a series elastic- and bowden cable-based actuation system for use as torque-actuator in exoskeleton-type training," in *IEEE, International Conference on Rehabilitation Robotics*, 2005, pp. 496 – 499.

[13] C. Acosta-Marquez and D. A. Bradley, "The analysis, design and implementation of a model of an exoskeleton to support mobility," in *IEEE, International Conference on Rehabilitation Robotics*, 2005, pp. 99 – 102.

[14] L. L. Cai, A. J. Fong, Y. Liang, J. Burdick, and V. Edgerton, "Assist-as-needed training paradigms for robotic rehabilitation of spinal cord injuries," in *Proceedings 2006 IEEE International Conference on Robotics and Automation*, 2006, pp. 3504 – 3511.

[15] B. Armstrong-Helouvry, P. Dupont, and C. C. D. Wit, "A survey of models, analysis tools and compensation methods for the control of machines with friction," *Automatica*, vol. 30, no. 7, pp. 1083 – 138, 1994.

[16] J. R. Garretson, W. T. Becker, and S. Dubowsky, "The design of a friction compensation control architecture for a heavy lift precision manipulator in contact with the environment," in *Proceedings 2006 IEEE International Conference on Robotics and Automation*, 2006, pp. 31– 36.

[17] A. Albu-Schaffer, W. Bertleff, B. Rebele, B. Schafer, K. Landzettel, and G. Hirzinger, "Rokviss - robotics component verification on iss current experimental results on parameter identification," in *Proceedings 2006 IEEE International Conference on Robotics and Automation*, 2006, pp. 3879 – 3885.

[18] M. Mahvash and A. M. Okamura, "Friction compensation for a force-feedback telerobotic system," in *Proceedings 2006 IEEE International Conference on Robotics and Automation*, 2006, pp. 3268 – 3273.

Appendix - Stability of Force-Field Controller

The force field controller applies tangential and normal forces on the foot based on the current position of the foot with respect to the desired trajectory. From the structure (Eq. 7) we can see that the foot can never come to rest, as at rest damping force (Eq. 6) is zero and the sum of tangential and normal forces never become zero. This is the result of the design of the controller to move the leg in a limit-cycle like pattern. However we can show that in the absence of the tangential force, the normal force can take the system to the nearest point $\mathbf{x}_{ref}$ on the desired trajectory.

On application of the force-field control law (7), the equations of motion (1) simplify to:

$$\mathbf{M}\ddot{\boldsymbol{\theta}} + \mathbf{C}(\dot{\boldsymbol{\theta}}, \boldsymbol{\theta})\dot{\boldsymbol{\theta}} = \mathbf{J}^T\mathbf{F} \tag{8}$$

$$\Rightarrow \mathbf{M}\ddot{\boldsymbol{\theta}} = -\mathbf{C}(\dot{\boldsymbol{\theta}}, \boldsymbol{\theta})\dot{\boldsymbol{\theta}} + \mathbf{J}^T\mathbf{F} \tag{9}$$

Choosing the lyapunov function as:

$$V = \frac{1}{2}\dot{\boldsymbol{\theta}}^T\mathbf{M}\dot{\boldsymbol{\theta}} + \frac{1}{2}\mathbf{x}_e^T\mathbf{P}\mathbf{x}_e \tag{10}$$

where $\mathbf{P}$ is a constant positive definite matrix. $\mathbf{x}_e$ is given by $\mathbf{x}_e = (x_e,\ y_e)^T = \mathbf{x}_{ref} - \mathbf{x}$. It can be seen from Eq. (10) that $V = 0$ only when $\dot{\boldsymbol{\theta}} = 0$ and $\mathbf{x}_e = 0$. Now differentiating V,

$$\dot{V} = \dot{\boldsymbol{\theta}}^T\mathbf{M}\ddot{\boldsymbol{\theta}} + \frac{1}{2}\dot{\boldsymbol{\theta}}^T\dot{\mathbf{M}}\dot{\boldsymbol{\theta}} - \dot{\mathbf{x}}^T\mathbf{P}\mathbf{x}_e \tag{11}$$

Substituting (9) in (11) and using $\dot{\mathbf{x}} = \mathbf{J}\dot{\boldsymbol{\theta}}$ and $\dot{\mathbf{x}}_e = -\dot{\mathbf{x}}$ gives:

$$\dot{V} = \frac{1}{2}\dot{\boldsymbol{\theta}}^T\left(\dot{\mathbf{M}} - 2\mathbf{C}\right)\dot{\boldsymbol{\theta}} + \dot{\boldsymbol{\theta}}^T\mathbf{J}^T\left(\mathbf{F} - K_d\mathbf{J}\dot{\boldsymbol{\theta}}\right) - \dot{\mathbf{x}}^T\mathbf{P}\mathbf{x}_e$$

Since $\dot{\mathbf{M}} - 2\mathbf{C}$ is skew symmetric, first term in above equation vanishes and is left with:

$$\dot{V} = -\dot{\boldsymbol{\theta}}^T\left(\mathbf{J}^T K_d\mathbf{J}\right)\dot{\boldsymbol{\theta}} + \dot{\boldsymbol{\theta}}^T\mathbf{J}^T\left(\mathbf{F} - \mathbf{P}\mathbf{x}_e\right)$$

First term in above equation is negative definite. To make $\dot{V} < 0$, we like to enforce $\mathbf{F} = \mathbf{P}\mathbf{x}_e$. $\mathbf{P}$ and $\mathbf{F}$ are chosen as:

$$\mathbf{P} = \begin{pmatrix} P_1 & 0 \\ 0 & P_2 \end{pmatrix} \quad \mathbf{F} = \begin{pmatrix} cF_1 \\ dF_2 \end{pmatrix}$$

c and d are additional parameter chosen in the following manner: $c = \frac{P_1 x_e}{F_1}$ and $d = \frac{P_2 y_e}{F_2}$. To enforce $\mathbf{F} = \mathbf{P}\mathbf{x}_e$. The choice of above parameters will take the foot towards the nearest point $\mathbf{N}$ on the desired trajectory. As shown in simulations and experiments, addition of tangential force takes the foot along the desired trajectory.